Characterization of *Caenorhabditis elegans* Homologs of the Down Syndrome Candidate Gene DYRK1A

William B. Raich,* Celine Moorman,† Clay O. Lacefield,* Jonah Lehrer,* Dusan Bartsch,* Ronald H. A. Plasterk,† Eric R. Kandel*,‡ and Oliver Hobert*,[1]

*Department of Biochemistry and Molecular Biophysics, Center for Neurobiology and Behavior, ‡Howard Hughes Medical Institute, Columbia University College of Physicians and Surgeons, New York, New York 10032 and †Hubrecht Laboratory, 3584 CT Utrecht, The Netherlands

Manuscript received June 18, 2002
Accepted for publication November 5, 2002

ABSTRACT

The pathology of trisomy 21/Down syndrome includes cognitive and memory deficits. Increased expression of the dual-specificity protein kinase DYRK1A kinase (DYRK1A) appears to play a significant role in the neuropathology of Down syndrome. To shed light on the cellular role of DYRK1A and related genes we identified three *DYRK/minibrain*-like genes in the genome sequence of *Caenorhabditis elegans*, termed *mbk-1*, *mbk-2*, and *hpk-1*. We found these genes to be widely expressed and to localize to distinct subcellular compartments. We isolated deletion alleles in all three genes and show that loss of *mbk-1*, the gene most closely related to DYRK1A, causes no obvious defects, while another gene, *mbk-2*, is essential for viability. The overexpression of DYRK1A in Down syndrome led us to examine the effects of overexpression of its *C. elegans* ortholog *mbk-1*. We found that animals containing additional copies of the *mbk-1* gene display behavioral defects in chemotaxis toward volatile chemoattractants and that the extent of these defects correlates with *mbk-1* gene dosage. Using tissue-specific and inducible promoters, we show that additional copies of *mbk-1* can impair olfaction cell-autonomously in mature, fully differentiated neurons and that this impairment is reversible. Our results suggest that increased gene dosage of human DYRK1A in trisomy 21 may disrupt the function of fully differentiated neurons and that this disruption is reversible.

TRISOMY of chromosome 21, or Down syndrome, is the most frequent chromosomal abnormality in human infants that come to term. Besides manifesting a characteristic set of facial and physical features, heart defects, and abnormalities in the immune and endocrine systems, patients with Down syndrome have deficits in spatial memory and difficulty in converting short-term to long-term memories (Johannsen *et al.* 1996; Takashima 1997). Although the cognitive defects of Down syndrome are likely to arise from increased dosage of many genes, several lines of evidence suggest that increased expression of the dual-specificity protein kinase DYRK1A plays a significant role. First, the DYRK1A locus maps to the Down syndrome candidate region (DSCR), a region of 70–100 genes (Shindoh *et al.* 1996). Rare patients with a partial trisomy of the DSCR display defects in cognition, suggesting that the genes in this region are sufficient to produce the cognitive defects of Down syndrome. Second, a 180-kb region on human chromosome 21 containing the DYRK1A locus is sufficient to produce defects in learning and memory in transgenic mice (Smith *et al.* 1997). Third, transgenic mice overexpressing the full-length *Dyrk1A* cDNA exhibit impairment in spatial learning and cognitive flexibility (Altafaj *et al.* 2001). The cellular and molecular consequences of these DYRK1A perturbations are unknown.

The first vertebrate member of the DYRK family was originally identified in a PCR screen for protein kinases (Kentrup *et al.* 1996) and subsequently shown to belong to a larger family of related dual-specificity kinases (Becker and Joost 1999) to which we refer here as the *DYRK/minibrain* family. Members of this family are localized to distinct subcellular compartments and phosphorylate various substrates *in vitro* (Becker and Joost 1999). They share the unusual property of tyrosine-directed autophosphorylation as well as phosphorylation of serine/threonine residues in exogenous substrates (Becker and Joost 1999). Their precise cellular role, however, remains elusive. Insights into their physiological relevance were provided by the finding that the Drosophila homolog of DYRK1A, termed *minibrain*, is involved in neuroblast proliferation in the fly brain (Tejedor *et al.* 1995). A similar reduction in brain size has been recently observed in DYRK1A knockout mice (Fotaki *et al.* 2002). The sole *Saccharomyces cerevisiae* representative of the *DYRK/minibrain* family, Yak1p, acts in parallel to a protein kinase A pathway to negatively regulate cell-cycle progression (Garrett and Broach 1989; Garrett *et al.* 1991).

In metazoan animals, the only *DYRK/minibrain* family

[1]*Corresponding author:* Columbia University, College of Physicians and Surgeons, 701 W. 168th St., HHSC 724, New York, NY 10032. E-mail: or38@columbia.edu

member for which mutant alleles exist is the Drosophila *minibrain* gene. Here, we describe the expression pattern and loss-of-function alleles of all three *DYRK/minibrain* family members in the nematode *Caenorhabditis elegans*. In contrast to Drosophila *minibrain*, we observe no obvious morphological defects in *mbk-1* mutants, but find that another *DYRK/minibrain* family member, *mbk-2*, is required for viability. In an attempt to model the cellular consequences of DYRK1A overexpression that are observed in Down syndrome patients, we analyzed the effects of providing extra copies of the worm ortholog of DYRK1A and describe dosage-sensitive and reversible defects in the processing of acute sensory information.

MATERIALS AND METHODS

cDNAs: A full-length *mbk-1* cDNA was amplified with SL1 and gene-specific primers. The structure of the cDNA is similar to the predicted T04C10.1 gene, with the exception of an incorrect first exon predicted in T04C10.1. The *mbk-2* locus generates two messages, a long form (*mbk-2L*) and a short form (*mbk-2S*) that uses an internal start site from an alternatively spliced exon. Both splice forms are represented in expressed sequence tag (EST) clones (a gift from Y. Kohara) that have been completely sequenced. Similarly, *hpk-1* full-length cDNA clones are represented in Y. Kohara's EST collection.

DNA constructs: Constructs are shown schematically in Figure 1.

mbk-1: To build *mbk-1::gfp*, the *mbk-1* genomic locus, including 7 kb of 5′ noncoding sequence and all exons and introns, was amplified by Expand long-template PCR (Boehringer Mannheim, Indianapolis). The PCR product was cloned in frame with *gfp* in the promoterless vector pPD95.75 (from A. Fire), generating pBR104. To build *mbk-1(YA)::gfp*, the QuickChange kit (Stratagene, La Jolla, CA) was used to modify pBR104 with primers YAs (5′-ctggacaccgaatcgcccaggccattcagt cgagattctatcg) and YAas (5′-cgatagaatctcgactgaatggcctgggcgat tcggtgtccag), generating pBR113. To build *mbk-1(pk1389)::gfp*, the *mbk-1* locus was amplified from homozygous *mbk-1(pk1389)* animals by Expand long-template PCR (Boehringer Mannheim). Following the cloning and sequencing of this PCR product, a 4.0-kb *Bgl*II-*Asp*718 fragment was subcloned into pBR104, generating pBR177. To build *pgcy-10::mbk-1*, the *gcy-10* promoter (Yu *et al.* 1997) was amplified from N2 genomic DNA by Expand long-template PCR (Boehringer Mannheim) and cloned in front of the full-length *mbk-1* cDNA, generating pBR145. To build *pgcy-10::mbk-1(YA)*, the QuickChange kit (Stratagene) was used to modify pBR145 with primers YAs and YAas, generating pBR147. To build *phsp16-2::mbk-1::gfp*, the full-length *mbk-1* cDNA was cloned into the heat-shock vector pPD49.78 (from A. Fire), generating pBR144. To generate a fusion with *gfp*, the promoter and cDNA were subsequently fused in frame with pBR104, generating pBR144.

mbk-2: To build *pmbk-2L::gfp*, 8 kb of 5′ noncoding sequence was amplified by Expand long-template PCR (Boehringer Mannheim) and cloned into pPD95.77 (from A. Fire), generating pBR126. To build *mbk-2S::gfp*, Expand long-template PCR (Boehringer Mannheim) was used to amplify exons 7–11 of the *mbk-2* locus and fused in frame with *gfp* in pPD95.77 (from A. Fire), generating pBR138. This construct uses intron 6 as the 5′ noncoding sequence. *pmbk-2L::gfp* and *mbk-2S* do not contain the full *mbk-2* genomic locus, and this may result in an artifactual or incomplete expression pattern. To build *phsp16-2::mbk-2L::gfp*, full-length *mbk-2L* cDNA was fused with *gfp* and inserted into the heat-shock vector pPD49.79 (from A. Fire), generating pBR169.

hpk-1: To build a translational fusion between HPK-1 and green fluorescent protein (GFP), the full-length *hpk-1* genomic locus, including 4 kb of 5′ noncoding sequence and all exons and introns, was amplified by Expand long-template PCR (Boehringer Mannheim) and cloned into the promoterless vector pPD95.77 (from A. Fire), generating pBR132.

Transgenic and mutant strains: The strains are as follows:

EK224 *cmIs6* [pBR104, pNC4.21] I; 6× outcrossed
EK270 *cmIs8* [pBR113, pNC4.21]; 2× outcrossed
EK176 *cmEx20* [pBR145, *unc-122::gfp*]
EK179 *cmEx21* [pBR147, *unc-122::gfp*]
EK173 *unc-4(e120)* II; *cmEx19* [pBR144, pNC4.21]
EK234 *unc-4(e120)* II; *cmEx31* [pBR169, pNC4.21]
EK123 *cmEx6* [pBR126, pRF4]
EK251 *cmEx16* [pBR138, pRF4]
EK135 *cmEx11* [pBR132, pRF4]
EK228 *mbk-1(pk1389)* X; 6× outcrossed
EK264 *cmEx36* [pBR177, pRF4]
EK273 *hpk-1(pk1393)* X; 6× outcrossed
EK275 *mbk-2(pk1427)/mgIs18* IV; 3× outcrossed

All expression constructs were injected at 50 ng/μl. pNC4.21 [*unc-4(+)*] and *unc-122::gfp* were injected at 50 ng/μl. pRF4 [*rol-6(d)*] was injected at 100 ng/μl. Integrated lines were obtained using a protocol described at http://cpmcnet.columbia.edu/dept/gsas/biochem/labs/hobert/integration_protocol.html.

Isolation of deletions in the *mbk-1*, *mbk-2*, and *hpk-1* loci: PCR screening of a chemically induced deletion library was done as previously described (Jansen *et al.* 1997). The relative position within the genomic loci of all three mutant alleles is schematically indicated in Figure 1. A 1658-bp deletion mutant of *mbk-1*, *pk1389*, was isolated using primers MBK1A (5′-gca gacgtgcctgacaatcttc) and MBK1D (5′-tgtaggtatggcggtatccgtc) and nested primers MBK1B (5′-ctcaaatacccagcaacactcac) and MBK1C (5′-caatagtagatcccatcctcag). The deleted PCR product from *pk1389* was sequenced and the deletion was confirmed by Southern analysis. The following sequence in capitals is deleted by *pk1389*: 5′-ataaaGCTTT-TTACGactat. The deletion extends from the first intron into the sixth exon. If in this context exon 1 is spliced to exon 7 (the beginning of the kinase domain), a frameshift and a premature stop would result; splicing of exon 1 to more downstream exons would also create frameshifts and/or delete the kinase domain. The *mbk-2* deletion, *pk1427*, spans 3398 bp in the genomic region represented in cosmid F49E11 and deletes the capitalized sequence 5′-tcgtcGTCCG-AAAACttgta. The *hpk-1* deletion, *pk1393*, spans 1457 bp in the genomic region represented in

Figure 1.—Reporter gene constructs and deletion alleles used to study *minibrain*-like genes. Boxes denote exons of the respective genes. Dark shaded bars above the genomic locus denote the location of the deletion in the respective mutant alleles (see materials and methods for precise location). Kinase domains are lightly shaded. The kinase domain was predicted using SMART (http://smart.embl-heidelberg.de/). The large size of the *mbk-2* genomic locus prevented us from constructing a full-length, translational *gfp* fusion construct. To monitor subcellular localization of *mbk-2* we thus fused the cDNA of the *mbk-2L* splice form to a heterologous promoter, *phsp16-2* (Fire *et al.* 1990). The two alternatively spliced *mbk-2* isoforms produced by the *mbk-2* locus were deduced by cDNA analysis (see materials and methods).

cosmid F20B6 and deletes the capitalized sequence 5′-caca cATGCC-TGACAtaatg. All deletion alleles lead to a disruption of the majority of the respective kinase domains and are predicted to act as null alleles.

RNAi: *mbk-2* dsRNA was delivered by bacterial feeding as previously described (Timmons *et al.* 2001). The effectiveness of RNAi could be assessed by monitoring the decrease in fluorescence of transgenic animals that expressed *gfp*-tagged *mbk-2*.

Behavioral assays: Chemotaxis assays toward volatile odor-

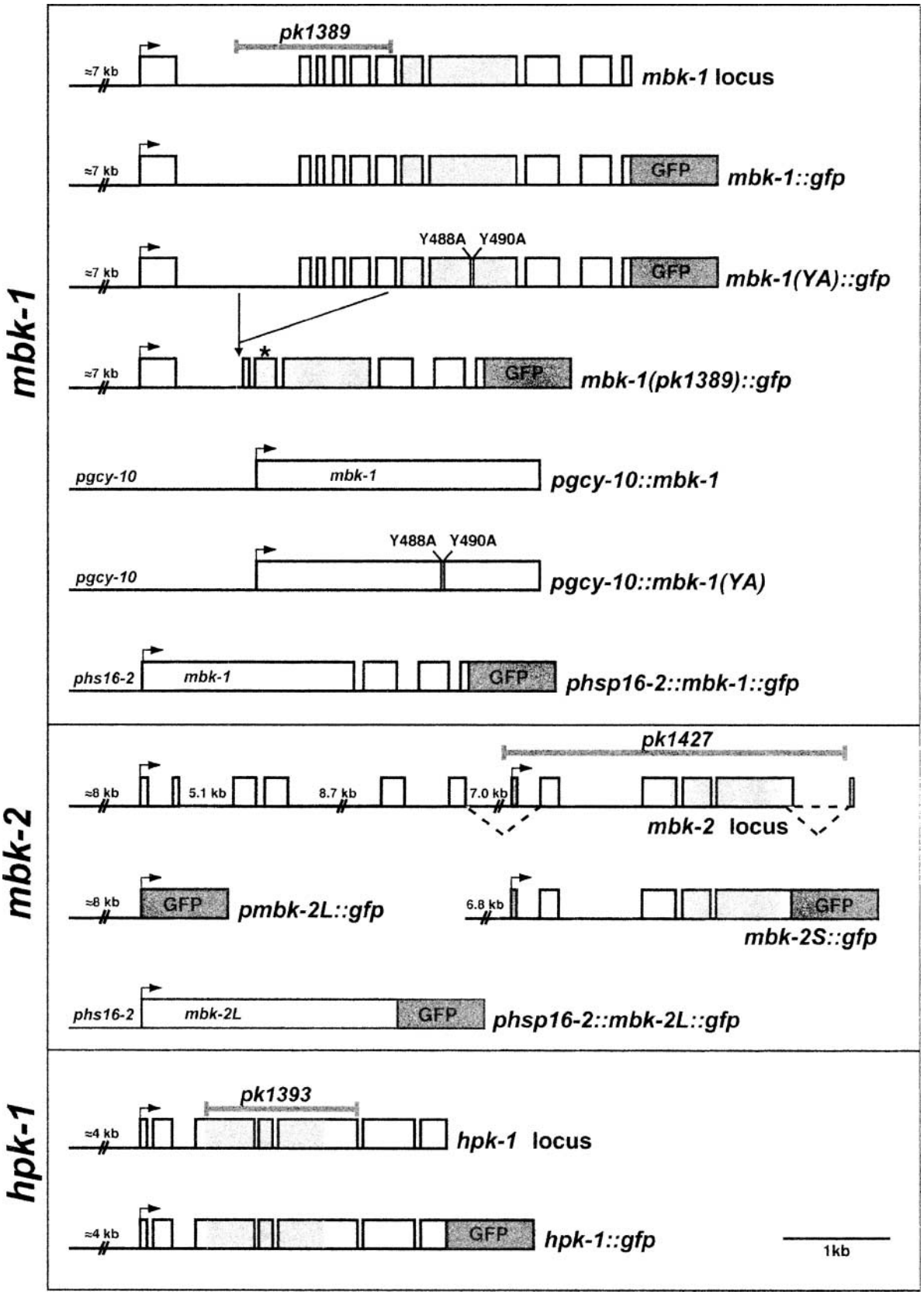

ants were performed as described (Bargmann *et al.* 1993). Chemotaxis index = (the number of animals attracted to the odorant) − (the number of animals at the opposite end of the plate)/(the total number of animals at both ends of the plate). When transgenic animals carrying extrachromsomal arrays were scored, only those animals that carry the injection marker were scored.

Scoring neuroanatomy: AWC morphology was observed by crossing *kyIs140,* a chromosomally integrated *str-2::gfp* construct (Troemel *et al.* 1999), into the respective mutant background. The generation, proliferation, and anatomy of several sensory neuron classes (ASK, ADL, ASI, AWB, ASH, ASJ, PHA, and PHB) were visualized by filling exposed sensory neurons with the lipophilic dye DiI, as previously described (Hedgecock *et al.* 1985). Briefly, a mixed population of well-fed worms was washed with M9 buffer, incubated at room temperature with 10 μg/ml DiI for 1 hr, washed several times with M9, and then mounted on a compound fluorescence microscope.

DAPI staining: 4′,6-Diamidino-2-phenylindole (DAPI) staining on *gfp*-expressing transgenic lines was done by placing animals in a drop of water on a coverslip, letting the water evaporate, adding a drop of acetone, letting the drop evaporate, drying for 20 min, and then adding 1 μg/ml DAPI in M9 medium.

RESULTS

Identification of *DYRK/minibrain*-like genes in *C. elegans*: Through sequence homology searching of the complete *C. elegans* genome sequence, we identified two *C. elegans* genes with close homology to the *DYRK/minibrain* family, termed *mbk-1* and *mbk-2* (for ***m**ini**b**rain-**k**inase*), and one gene, *hpk-1* (named after its vertebrate homologs, ***h**omeodomain-**i**nteracting **p**rotein **k**inase **1-3***), with a more distant homology (Figure 2A). *mbk-1* and *mbk-2* both carry the characteristic DYRK family signature motifs in their kinase domain, as well as a DH-box, a conserved sequence motif preceding the catalytic domain (Becker and Joost 1999). *mbk-1* is unique among the *C. elegans DYRK/minibrain* family members in clustering in the DYRK1A subgroup (Figure 2A). In addition to highest overall sequence similarity, MBK-1 and DYRK1A can also be distinguished from other DYRK family members by their sharing of an N-terminal nuclear localization sequence, a leucine zipper in the kinase domain, and stretches of homopolymeric amino acids at their C termini (Figure 2B). We thus consider MBK-1 the *C. elegans* ortholog of human DYRK1A.

Expression and subcellular localization of *DYRK/minibrain*-like genes in *C. elegans*: To determine the sites of expression and subcellular localization of *DYRK/minibrain*-like genes, we fused *gfp* in frame with the respective genomic loci (Figure 1). The *mbk-1::gfp* construct included 7 kb of 5′ noncoding sequence and all of the exons and introns present in the endogenous *mbk-1* locus. The *mbk-1::gfp* gene product is expressed in all somatic cells and primarily localizes to nuclei (Figure 3), similar to the reported expression and subcellular localization of human DYRK1A (Song *et al.* 1997; Becker *et al.* 1998). During development, *mbk-1::gfp* expression can first be observed around the 300-min stage, when

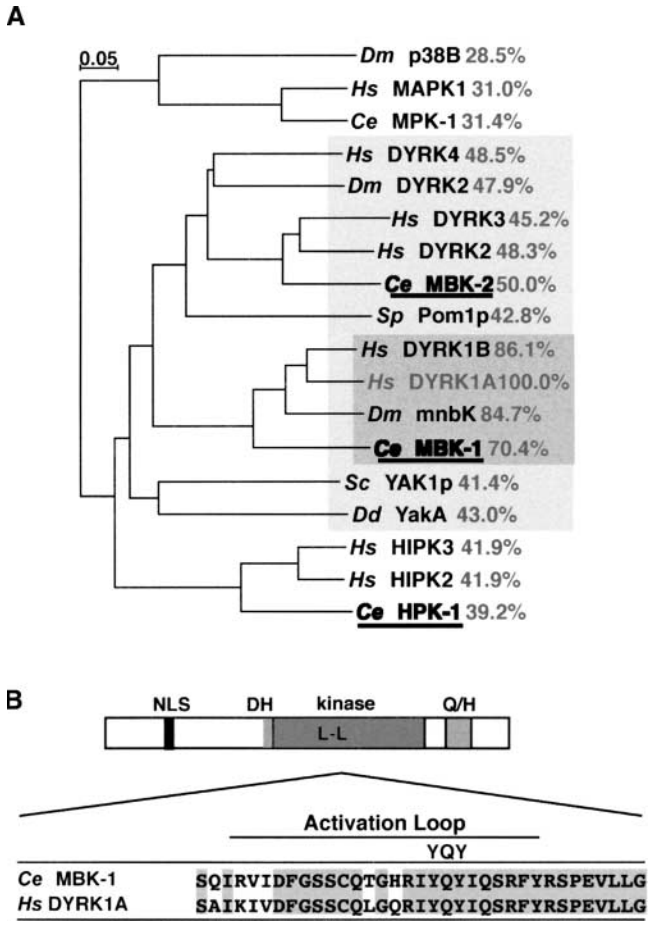

Figure 2.—The *DYRK/minibrain*-like gene family in *C. elegans.* (A) Classification of the DYRK subfamily of protein kinases. On the basis of BLAST- and PFAM-based similarity searches of the complete genome sequence, *C. elegans* has two members of the DYRK subfamily of protein kinases, MBK-1 (T04C10.1; LGX; GenBank accession no. AY064464) and MBK-2 (F49E11.1; LGIV; GenBank accession no. AY090019), as well as a related kinase called HPK-1 (F20B6.8; LGX). The gene structures of *mbk-1* and *mbk-2* were confirmed by sequence analysis of EST clones. The alignment and dendrogram were generated from the predicted kinase domains using ClustalX and Align with default parameters. The DYRK1A group is boxed by dark shading, the DYRK subfamily is boxed by light shading, *C. elegans* proteins are in boldface type and underlined, and the percentage identity between each kinase domain and that of DYRK1A is listed to the right. (B) MBK-1 is the closest homolog to DYRK1A, whose overexpression is implicated in Down syndrome. The relative positions of the N-terminal nuclear localization sequence [NLS; amino acids (aa) 120–127], the DH box, the kinase domain (aa 317–649), leucine zipper (L-L; aa 443–464; contains four leucines each spaced by 6 aa), and C-terminal homo-polymeric stretch of amino acids (histidines in DYRK1A, glutamines in MBK-1) sites are shown. DYRK kinases are regulated through the phosphorylation of two DYRK-specific tyrosines within the activation loop (Y-Y; aa 488 and 490). For a more detailed alignment and more sequence features of DYRK kinases, see Becker and Joost (1999).

cell division ceases and morphogenesis begins (Figure 3A). Expression levels increase during later embryonic stages and remain at comparable levels throughout larval and adult stages (Figure 3).

In contrast to *mbk-1*, *mbk-2::gfp* reporter constructs were expressed in subsets of tissues, including the nervous system, body wall muscle, and the pharynx (Figure 4, A–C). To determine the subcellular localization of MBK-2 protein, we fused a cDNA—encoding the longer splice form of *mbk-2* (see Figure 1 and MATERIALS AND METHODS)—to *gfp* and expressed it under control of a ubiquitously expressed promoter (Figure 1). Unlike MBK-1::GFP, but like its vertebrate ortholog DYRK2 (BECKER *et al.* 1998), MBK-2::GFP was excluded from the nucleus (Figure 4D).

A translational HPK-1::GFP reporter construct (Figure 1) was broadly expressed during embryogenesis and localized to moving nuclear puncta (Figure 4, E–H). In adult animals, the number, intensity, and movement of HPK-1-GFP puncta are greatly reduced. Although we have not further examined the identity of these puncta, the observation that the three vertebrate homologs of HPK-1, HIPK1–3, stably bind and phosphorylate nuclear transcription factors (KIM *et al.* 1998) suggests that these dots may represent sites of active transcription.

Taken together, the distinctive subcellular localization patterns described here for the individual *C. elegans DYRK/minibrain* family members reveal a striking similarity to their presumptive vertebrate orthologs and, together with the primary sequence similarity, suggests that vertebrate and *C. elegans DYRK/minibrain* proteins fulfill similar functions.

Providing extra copies of *mbk-1* causes dosage-sensitive olfactory defects: Because human DYRK1A overexpression has been implicated in the behavioral defects of Down syndrome, we wanted to examine the consequences of overexpression of the DYRK1A ortholog *mbk-1* on *C. elegans* behavior. Toward this end, a multicopy array derived from a subcloned amplicon of the *mbk-1* genomic locus was integrated into the genome of wild-type worms, giving rise to multiple independent lines that harbor additional copies of *mbk-1* (see Figure 1 for constructs). An appended *gfp* tag allowed us to monitor ectopic *mbk-1* expression, which we observed broadly throughout the whole animal (Figure 3). In light of the multicopy nature of stably transmitted DNA arrays in *C. elegans* (MELLO *et al.* 1991), the level of ectopic *mbk-1* expression is possibly significantly greater than the 1.5-fold DYRK1A overexpression resulting from trisomy 21; however, as we have no means of assessing expression of endogenous MBK-1 protein we cannot conclusively state that we "overexpress" *mbk-1*, but we can clearly state, on the basis of the appended *gfp* tag, that we provided extra copies of the *mbk-1* gene.

All of the transgenic lines that contain extra copies of

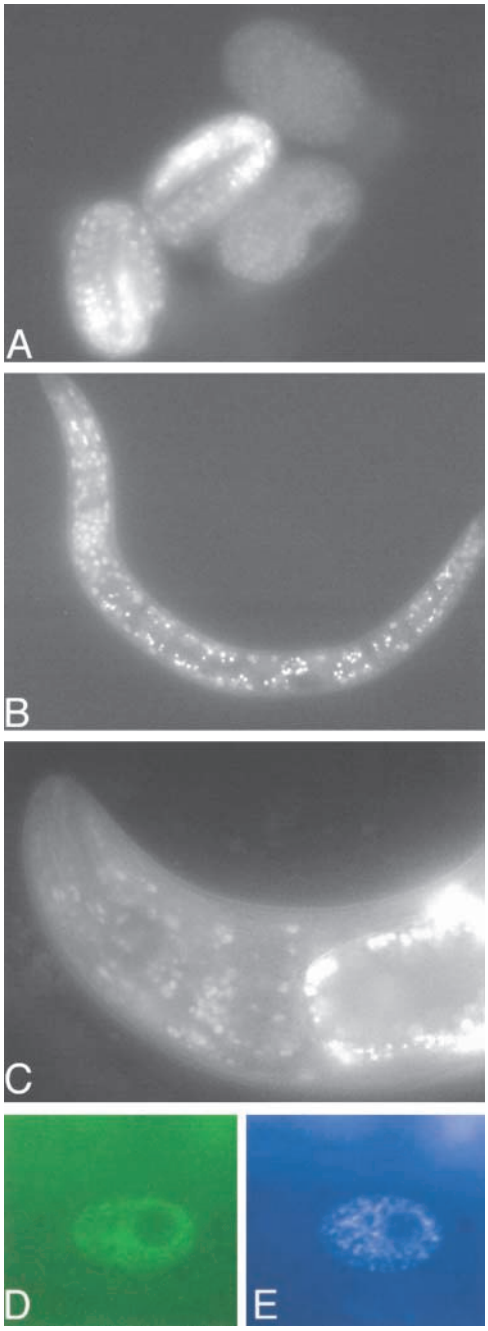

FIGURE 3.—Expression of the *DYRK1A/minibrain* ortholog *mbk-1* gene as assayed by reporter gene analysis. MBK-1::GFP is expressed in all somatic tissues and primarily localizes to nuclei in embryos (A), larvae (B), and adults (C). Nuclear localization can be observed in all cells and is particularly obvious in the enlarged nuclei of hypodermal cells (D, MBK-1::GFP; E, DAPI staining; the dark center is the nucleolus). Expression is monitored from a chromosomally integrated array, *cmIs6*. (A) Embryos at different stages; the embryo at the top is roughly at 300 min of development entering morphogenesis and showing the first signs of *mbk-1::gfp* expression; the embryo on the lower left is at the comma stage with slightly increased *mbk-1::gfp* expression. Maximal levels of *mbk-1::gfp* expression are then observed around threefold stages (embryos on left).

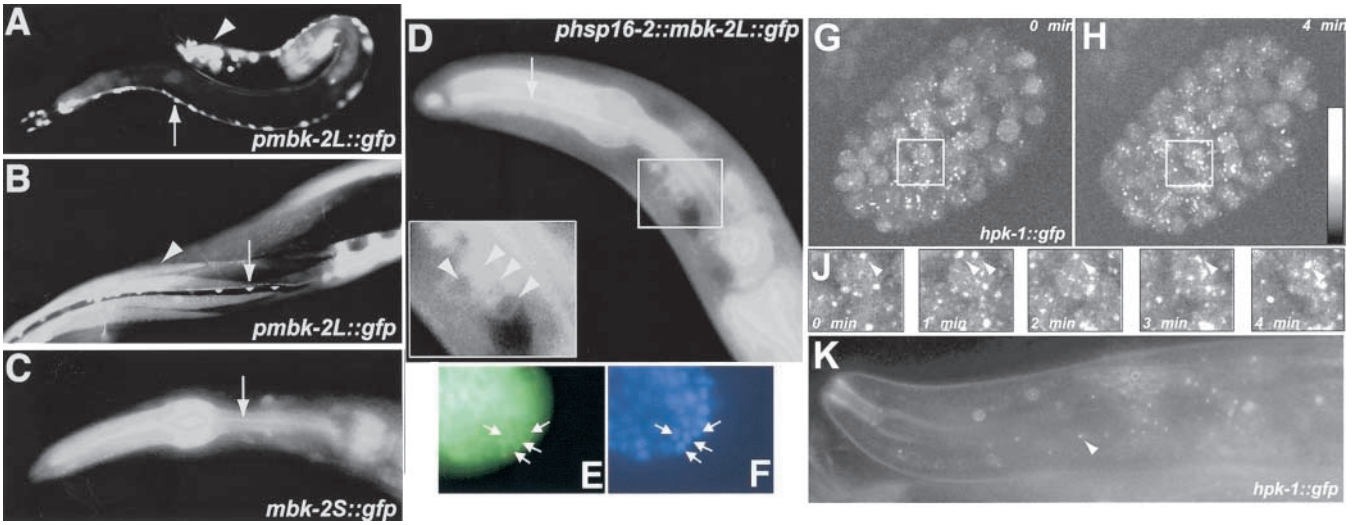

Figure 4.—Expression of other DYRK1A/minibrain family members. (A–F) MBK-2::GFP is excluded from the nucleus and is expressed in the nervous system. Expression constructs are shown in Figure 1. (A) In L1 larvae, the 5′ noncoding sequence of *mbk-2L* drives *gfp* expression widely in the nervous system, including head neurons (arrowhead) and the ventral nerve cord (arrow). (B) In adult animals, *gfp* continues to be expressed in the nervous system (arrow) and is also expressed in body wall muscle (arrowhead). (C) A translational fusion between *mbk-2S* and *gfp* is expressed at the periphery of the pharynx (arrow). (D) Induced expression of a translational fusion protein between *mbk-2L* and *gfp* also localizes to the periphery of the pharynx (arrow). In addition, the protein is clearly excluded from the nuclei of neurons in the head (inset, arrowheads); nuclear exclusion was further corroborated by DAPI staining of an embryo (F) that expresses *mbk-2::gfp* (E). (G–K) HPK-1::GFP expression. The expression construct is shown in Figure 1. To monitor GFP expression in living embryos, two-photon laser scanning microscopy was used on mounted embryos. (G) A translational fusion protein between *hpk-1* and *gfp* localizes to nuclei and is widely expressed in cleavage stage embryos. (H) After 4 min, the number and location of HPK-1-GFP puncta within the embryo has dramatically changed. (J) The boxed region is shown at 1-min intervals. The puncta within the highlighted nucleus rapidly rearrange (arrowheads). (K) A fluorescence micrograph of HPK-1-GFP at postembryonic stages. In adult animals, the number, intensity, and movement of HPK-1-GFP puncta (arrowhead) are greatly reduced.

mbk-1, here on referred to as *mbk-1(gf)* animals, appeared normal in respect to overall morphology, life span, dauer formation, thermotaxis, mechanosensation, and chemotaxis toward water-soluble attractants (data not shown). *mbk-1(gf)* animals display no defects in locomotory rate or reversal behavior (data not shown). However, olfaction toward several volatile chemoattractants was markedly disrupted in *mbk-1(gf)* animals (Figure 5). Comparable defects were observed with chromosomally integrated lines that contain extra copies of either wild-type *mbk-1* or a mutated version of *mbk-1* in which the kinase activity was potentially hyperactivated (Y-to-E change in kinase domain; data not shown). *mbk-1(gf)* defects are apparent throughout a wide range of odor concentrations.

The olfactory-defective phenotype was sensitive to gene dosage, since animals heterozygous for the integrated *mbk-1* array display intermediate odortaxis defects. As a control, we provided extra copies of *mbk-1*, again under the control of its own promoter and tagged with *gfp* to monitor expression, but containing an inactivated kinase domain (Figure 1). We found that worms containing integrated copies of the *mbk-1(YA)* genomic construct showed no defects in odortaxis (Figure 5A). Additional copies of *mbk-2* also produced no olfaction defect (Figure 6B). All ectopic expression constructs yielded comparable levels of protein expression as assessed by the added GFP tag. The olfaction phenotype thus requires the kinase activity of *mbk-1*, is specific to *mbk-1*, and is sensitive to gene dosage.

Attractive olfactory responses in *C. elegans* are largely mediated by two bilaterally symmetric pairs of ciliated sensory neurons, called AWA and AWC (Bargmann *et al.* 1993). These neurons are capable of sensing a wide variety of discrete odorants. We found that extra copies of *mbk-1* strongly inhibited odortaxis toward AWC-sensed odorants such as benzaldehyde, isoamylalcohol, and 2-butanone across a wide range of concentrations (Figure 5B). In contrast, extra copies of *mbk-1* caused only marginal defects in the response to AWA-sensed odorants such as diacetyl and pyrazine (Figure 5B).

The cellular specificity of odortaxis defects induced by extra copies of *mbk-1* agrees with our observation that *mbk-1(gf)* animals are indistinguishable from wild-type animals in all other behaviors tested and suggests that *mbk-1* acts selectively within specific cellular contexts rather than affecting neuronal signaling in a broad and unspecific way.

***mbk-1* can act autonomously in sensory neurons:** To elucidate the cellular context in which extra copies of *mbk-1* can affect olfactory behavior, we added extra copies of *mbk-1* specifically in olfactory neurons using the

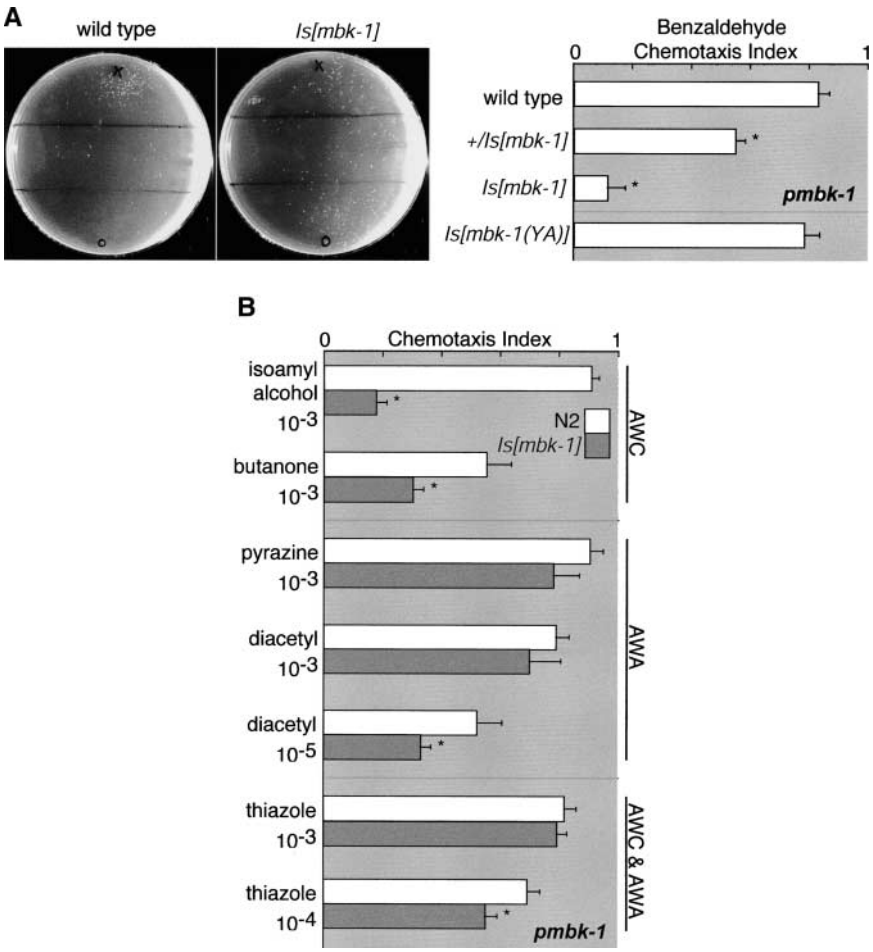

FIGURE 5.—Extra copies of *mbk-1* produce defects in chemotaxis to volatile attractants. (A) Odortaxis to benzaldehyde, which is sensed mainly by AWC chemosensory neurons. Representative odortaxis plates are shown for wild type (N2) and animals that are homozygous for an integrated multicopy *mbk-1* array (*Is[mbk-1]* = *cmIs6*). Odortaxis results with wild-type animals and animals that are homozygous (*Is[mbk-1]*) and heterozygous (+/*Is[mbk-1]*) for extra copies of wild-type *mbk-1* arrays and homozygous for kinase-inactivated *mbk-1* arrays (*Is[mbk-1(YA)]* = *cmIs8*) are shown. Tyrosines 488 and 490 were mutated to alanine in kinase-inactivated MBK-1, since equivalent tyrosines in DYRK1A are essential for kinase activity (KENTRUP *et al.* 1996; HIMPEL *et al.* 2001). The *mbk-1(YA)* construct was also tagged with *gfp* and expression levels were found to be indistinguishable from those of animals that express extra copies of wild-type *mbk-1*. For a summary of expression constructs see Figure 1. (B) The response to odorants sensed by the AWC chemosensory neurons (isoamylalcohol, 2-butanone) is affected more strongly by providing extra copies of *mbk-1* than the response to odorants sensed by the AWA chemosensory neurons (pyrazine, diacetyl) or by both AWC and AWA (2,4,5-trimethylthiazole). N2 (open bars) and *Is[mbk-1]* (shaded bars) are shown. Each bar represents at least five independent assays; error bars show SEM and an asterisk indicates that the values differ significantly ($P < 0.05$) from controls.

gcy-10 promoter, which is active in the AWC and AWB chemosensory neurons, as well as in the pharyngeal interneuron I1 (YU *et al.* 1997; Figure 1). As a control, kinase-inactivated *mbk-1* was also expressed under control of the *gcy-10* promoter (Figure 6A). Transgenic lines expressing wild-type *mbk-1* in AWB/C/I1 showed impaired odortaxis toward benzaldehyde, sensed by AWC (Figure 6A), but normal odortaxis toward diacetyl, sensed by AWA (data not shown). In contrast, transgenic lines expressing kinase-inactivated *mbk-1* in AWB/C/I1 displayed normal odortaxis toward both benzaldehyde and diacetyl. Because AWB is dispensable for chemotaxis toward volatile attractants (BARGMANN *et al.* 1993), and because the pharyngeal neuron I1 is primarily isolated from the somatic nervous system (ALBERTSON and THOMSON 1976), these results suggest that *mbk-1* overexpression can act cell-autonomously in AWC to disrupt neuronal function. The disruption in odortaxis is less severe in animals expressing *mbk-1* under control of the *gcy-10* promoter than in animals expressing *mbk-1* under control of its own promoter or of the heat-shock promoter. This may arise because *gcy-10* is a relatively weak promoter or because additional copies of *mbk-1* provided under control of its own ubiquitous promoter disrupt the function not only of AWC but also of other cells (such as, for example, in downstream interneurons).

***mbk-1* can act reversibly and acutely in differentiated neurons:** Given that odortaxis defects arise from increasing *mbk-1* gene dosage, an important issue is determining the temporal window of *mbk-1* function: Is the increased gene dosage altering development or the function of already differentiated cells? To address this issue, we followed several approaches: First, we tested whether AWC development is affected in *mbk-1(gf)* mutants by assessing AWC generation, proliferation, or anatomy using *str-2::gfp* (TROEMEL *et al.* 1999) as an anatomical marker (Figure 7). We observed no obvious abnormalities. Moreover, the characteristic left/right asymmetric expression of the *str-2* marker, a sensitive indicator of function and development of the left/right AWC neuron pair (TROEMEL *et al.* 1999), is unaffected in *mbk-1(gf)* animals. As a second approach to delineate *mbk-1* function, we used the inducible heat-shock promoter *hsp 16-2* (FIRE *et al.* 1990) to drive expression of an *mbk-1* cDNA fused to *gfp*. Adult animals that received a dose of *mbk-1* expression during embryogenesis and the first larval stage, steps in which the cells and structures essential for chemotaxis differ-

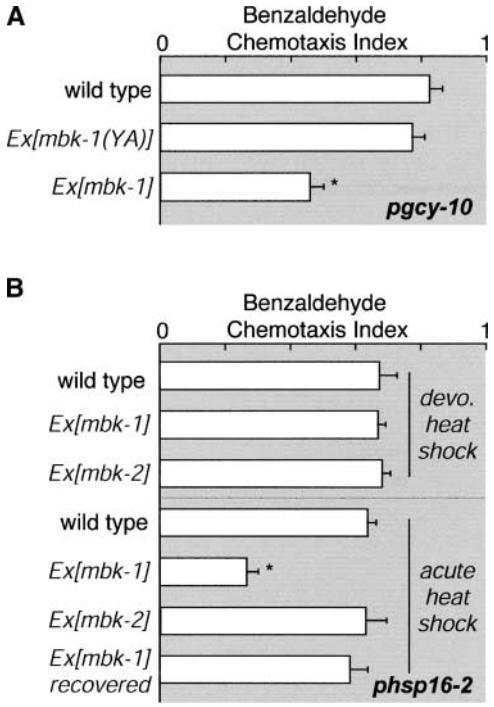

FIGURE 6.—*mbk-1(gf)* acts reversibly and acutely in differentiated neurons. (A) Odortaxis to benzaldehyde of wild-type animals (N2) and animals that express *mbk-1* (*Ex[mbk-1]*) and kinase-inactivated *mbk-1* (*Ex[mbk-1(YA)]*) under control of the *gcy-10* promoter. (B) Odortaxis to benzaldehyde. *mbk-1* or *mbk-2* was fused with *gfp* and expressed using the inducible promoter *hsp 16-2* (FIRE *et al.* 1990). To developmentally stage the heat shocks, gravid hermaphrodites were collected and treated with alkaline hypochlorite to physically separate the embryos. For the developmental heat shocks (*devo. heat shock*), these embryos were immediately placed at 33° for 1 hr, returned to 20° for 12 hr, heat-shocked again for 1 hr, and allowed to grow to adulthood at 20° prior to the assay. For adult expression, young adult animals were heat-shocked at 33° for 1 hr, returned to 20° for 2 hr, and assayed either immediately (*acute heat shock*) or following 24 hr (*recovered*). On the basis of GFP fluorescence, MBK-1::GFP or MBK-2::GFP were expressed for >12 hr but <24 hr following 1 hr at 33° and both were expressed at approximately similar levels. Each bar represents at least five independent assays; error bars show SEM and an asterisk indicates that the values differ significantly ($P < 0.05$) from controls.

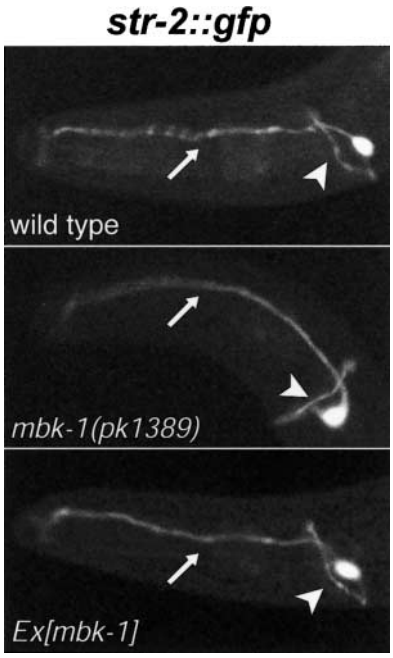

FIGURE 7.—Decreases or increases in *mbk-1* gene function do not affect olfactory neuron proliferation or differentiation. *str-2::gfp(kyIs140)* was used to examine the morphology of the AWC neurons in *mbk-1(pk1389)* and *mbk-1(gf)* animals. The dendrites (arrows) and axons (arrowheads) showed no gross morphological abnormalities following *mbk-1* perturbation. In addition, the left/right asymmetrical expression of *str-2::gfp* was preserved. Other neurons also show no proliferation defects (data not shown).

entiate, showed a normal response to the AWC-sensed odorant benzaldehyde (Figure 6B and data not shown). In contrast, adult animals in which *mbk-1* expression was induced 2 hr before the assay showed a significant decrease in odortaxis toward benzaldehyde. Extra copies of *mbk-2*, whose expression was also monitored with an attached *gfp* tag (Figure 1), produced no defects (Figure 6B).

Intriguingly, the effects of providing extra copies of *mbk-1* overexpression were reversible, since adult animals tested 24 hr after *mbk-1* induction displayed normal olfaction (Figure 6B; note that decrease in *mbk-1* expression could be monitored with the attached *gfp* tag). These results indicate that extra copies of *mbk-1* interfere with the acute function, but not with the formation or differentiation, of the olfactory neurons and that the phenotypes resulting from overexpressed *mbk-1* can be reversed by reducing *mbk-1* levels.

Loss-of-function analysis of *mbk-1*: The defects caused by providing additional copies of *mbk-1* prompted us to elucidate the *mbk-1* loss-of-function phenotype. We isolated a *mbk-1* loss-of-function allele, *pk1389*, through PCR screening of a *C. elegans* deletion library. *pk1389* is a likely null allele since it eliminates exons 2–6 of *mbk-1*. Exon splicing around this deletion would lead to a frameshift and to a premature stop in the message or to a deletion of the entire kinase domain (Figure 1 and MATERIALS AND METHODS). To confirm this notion, we introduced the *pk1389* deletion into the context of the translational *mbk-1::gfp* construct (Figure 1) and found that transgenic animals expressing this construct show no *gfp* expression (data not shown).

mbk-1(pk1389) homozygous mutant animals are viable and show no obvious morphological abnormalities. We examined several aspects of nervous system function in *mbk-1* mutants, including the behavior of *mbk-1* mutants in response to various sensory inputs (mechano- and chemosensory), and detailed aspects of its locomotory behavior. We observed no obvious defects under standard conditions (data not shown). We observed slight

but significant defects in attraction to low doses of olfactory cues, but since we were not able to rescue this phenotype through expression of *mbk-1* from extrachromosomal arrays, we could not conclude that these defects are indeed due to loss of *mbk-1* (data not shown; these rescue experiments may have failed because of an inability to supply precisely the right amount of *mbk-1*).

We examined nervous system architecture of *mbk-1* mutant animals in more detail. We visualized a total of 18 individual head and tail sensory neurons and their axonal anatomy in the main head ganglia of *C. elegans* both with *gfp* reporter genes that label individual cells and with the fluorescent dye DiI (Hedgecock *et al.* 1985) and found no morphological defects or aberrant cell numbers in *mbk-1(lf)* mutants (Figure 7 and data not shown). Since most of these 18 visualized neurons derive nonclonally from different embryonic precursors (ABalp, ABpla, ABplp, Abpra, and ABprp), their visualization allowed us to ascertain the integrity of various lineage branches in *mbk-1* mutants. The absence of any defects in cell generation and number is significant in light of the widespread neuroblast proliferation defects that lead to a significantly reduced brain size observed in Drosophila *minibrain* mutants (Tejedor *et al.* 1995).

Isolation of loss-of-function alleles in other *DYRK1A/minibrain* family members: Since *mbk-1* may act redundantly with other *DYRK1A/minibrain* family members to affect *C. elegans* nervous system development or function, we isolated mutations in the only other two *DYRK1A/minibrain*-related genes in the *C. elegans* genome, namely *mbk-2* and *hpk-1* (Figures 1 and 2). Due to their deletion of the respective kinase domains, the *mbk-2* and *hpk-1* mutant alleles constitute likely null alleles (Figure 1).

While *hpk-1* null mutant animals are viable and appear indistinguishable from wild type (data not shown), *mbk-2(pk1427)* homozygous animals display 100% penetrant maternal-effect embryonic lethality. The maternal-effect lethality is caused by defects in spindle positioning and cytokinesis in the early embryo (J. Pellettieri and G. Seydoux, personal communication). In addition, *mbk-2* homozygous animals derived from a heterozygous parent appear sick and grow poorly. To independently confirm the linkage of the lethality with the *mbk-2* locus, we inactivated *mbk-2* by RNAi (Fire *et al.* 1998) and observed 100% embryonic lethality in the progeny of 7 out of 10 adult *mbk-2(RNAi)* animals and >80% embryonic lethality in the progeny of the remaining 3 animals. The survivors display vulval defects at low penetrance (11%; data not shown). The embryonic lethality and overall sickness of maternally rescued *mbk-2* mutant animals did not allow us to test whether *mbk-1* and *mbk-2* have redundant functions in nervous system function.

DISCUSSION

Our analysis of the *C. elegans* homologs of the *DYRK/minibrain* family of protein kinases reveals strong patterns of similarity in expression and subcellular localization of these proteins across phylogeny. Like their vertebrate orthologs, all three *DYRK/minibrain*-like genes are broadly expressed. MBK-1, like its vertebrate ortholog DYRK1A, localizes to the nucleus while the closely related MBK-2, like its vertebrate ortholog DYRK2, is predominantly cytoplasmic and excluded from the nucleus. HPK-1, like its vertebrate homolog HIPK2, is localized to subnuclear puncta. However, interspecies comparisons in mutant phenotypes reveal a strong dissimilarity. While the Drosophila *minibrain* locus affects neuroblast proliferation and hence brain size (Fischbach and Heisenberg 1984; Tejedor *et al.* 1995), a physiological function apparently conserved in mice (Fotaki *et al.* 2002), we observed no apparent cellular proliferation defects in the nervous system of *mbk-1* mutant animals. Our mutant analysis of the other two *DYRK/minibrain*-like genes, none of which have been knocked out in any other species, revealed that one of them, *mbk-2*, is essential for viability, due to a function of the gene in cytokinesis in the early embryo (J. Pellettieri and G. Seydoux, personal communication); perhaps this defect relates to the neuroblast proliferation defects in Drosophila *minibrain* mutants. However, *mbk-1*, and not *mbk-2*, represents the Drosophila sequence ortholog of *minibrain* and Drosophila has a separate *mbk-2*-orthologous gene (Figure 2).

The most important conclusions from our functional analysis of *DYRK1/minibrain* family genes derive from providing extra copies of the *mbk-1* gene. First, increases in *mbk-1* expression produce functional olfactory defects without apparently interfering with either neuronal proliferation or neuronal differentiation. Second, the phenotypes resulting from providing extra copies of *mbk-1* can be specifically induced in adult animals and are thus acute rather than developmental defects. Third, the defects can be reversed by restoring *mbk-1* to normal levels of expression. Fourth, extra copies of the ubiquitously expressed *mbk-1* gene specifically disrupt olfactory behavior but no other behaviors tested. This apparent specificity suggests that additional copies of *mbk-1* do not cause an unspecific disruption of signaling or sickening of a neuron, but act in a cellular-context-dependent manner.

We conclude that aberrant expression levels of *mbk-1* interfere with acute sensory processing in olfactory neurons. This finding is relevant since it is the additional copy of the vertebrate *mbk-1* ortholog DYRK1A that causes neurological defects either in humans or in mouse models. Our experiments with the temporal regulation and reversibility of *mbk-1* expression phenotypes may be taken as an indication that human DYRK1A overexpression disrupts the function of terminally differentiated neurons. Moreover, the reversibility of defects observed upon the reversion of *mbk-1* expression levels back to normal suggests that therapies aimed at the reduction of DYRK1A expression or activity may provide a viable

therapeutic approach for the neurological defects of Down syndrome.

We thank Y. Kohara (National Institute for Genetics, Mishima, Japan) for cDNA clones, A. Fire (Carnegie Institution, Baltimore) for vectors, members of the worm community for plasmids and strains, G. Seydoux for communicating unpublished results, and the *Caenorhabditis* Genetics Center for the nematode strains used in this study. We are grateful to Iva Greenwald, Piali Sengupta, and members of the Kandel and Hobert labs for helpful comments during the preparation of this manuscript and to Kelvin Pau and Ephraim Tsalik for help with performing several behavioral assays. This work was funded by the Howard Hughes Medical Institute, National Institutes of Health postdoctoral fellowship 5 F32 NS11114 to W.B.R., The Netherlands Organization for Scientific Research, and the Klingenstein, Rita Allen, Hirschl, Sloan, McKnight, and Whitehall Foundations (O.H.).

LITERATURE CITED

Albertson, D. G., and J. N. Thomson, 1976 The pharynx of Caenorhabditis elegans. Philos. Trans. R. Soc. Lond. B Biol. Sci. **275:** 299–325.

Altafaj, X., M. Dierssen, C. Baamonde, E. Marti, J. Visa *et al.*, 2001 Neurodevelopmental delay, motor abnormalities and cognitive deficits in transgenic mice overexpressing Dyrk1A (minibrain), a murine model of Down's syndrome. Hum. Mol. Genet. **10:** 1915–1923.

Bargmann, C. I., E. Hartwieg and H. R. Horvitz, 1993 Odorant-selective genes and neurons mediate olfaction in C. elegans. Cell **74:** 515–527.

Becker, W., and H. G. Joost, 1999 Structural and functional characteristics of Dyrk, a novel subfamily of protein kinases with dual specificity. Prog. Nucleic Acid Res. Mol. Biol. **62:** 1–17.

Becker, W., Y. Weber, K. Wetzel, K. Eirmbter, F. J. Tejedor *et al.*, 1998 Sequence characteristics, subcellular localization, and substrate specificity of DYRK-related kinases, a novel family of dual specificity protein kinases. J. Biol. Chem. **273:** 25893–25902.

Fire, A., S. W. Harrison and D. Dixon, 1990 A modular set of lacZ fusion vectors for studying gene expression in Caenorhabditis elegans. Gene **93:** 189–198.

Fire, A., S. Xu, M. K. Montgomery, S. A. Kostas, S. E. Driver *et al.*, 1998 Potent and specific genetic interference by double-stranded RNA in Caenorhabditis elegans. Nature **391:** 806–811.

Fischbach, K. F., and M. Heisenberg, 1984 Neurogenetics and behavior in insects. J. Exp. Biol. **112:** 65–93.

Fotaki, V., M. Dierssen, S. Alcantara, S. Martinez, E. Marti *et al.*, 2002 Dyrk1A haploinsufficiency affects viability and causes developmental delay and abnormal brain morphology in mice. Mol. Cell. Biol. **22** (18): 6636–6647.

Garrett, S., and J. Broach, 1989 Loss of Ras activity in Saccharomyces cerevisiae is suppressed by disruptions of a new kinase gene, YAKI, whose product may act downstream of the cAMP-dependent protein kinase. Genes Dev. **3:** 1336–1348.

Garrett, S., M. M. Menold and J. R. Broach, 1991 The Saccharomyces cerevisiae YAK1 gene encodes a protein kinase that is induced by arrest early in the cell cycle. Mol. Cell. Biol. **11:** 4045–4052.

Hedgecock, E. M., J. G. Culotti, J. N. Thomson and L. A. Perkins, 1985 Axonal guidance mutants of Caenorhabditis elegans identified by filling sensory neurons with fluorescein dyes. Dev. Biol. **111:** 158–170.

Himpel, S., P. Panzer, K. Eirmbter, H. Czajkowska, M. Sayed *et al.*, 2001 Identification of the autophosphorylation sites and characterization of their effects in the protein kinase DYRK1A. Biochem. J. **359:** 497–505.

Jansen, G., E. Hazendonk, K. L. Thijssen and R. H. Plasterk, 1997 Reverse genetics by chemical mutagenesis in Caenorhabditis elegans. Nat. Genet. **17:** 119–121.

Johannsen, P., J. E. Christensen and J. Mai, 1996 The prevalence of dementia in Down syndrome. Dementia **7:** 221–225.

Kentrup, H., W. Becker, J. Heukelbach, A. Wilmes, A. Schurmann *et al.*, 1996 Dyrk, a dual specificity protein kinase with unique structural features whose activity is dependent on tyrosine residues between subdomains VII and VIII. J. Biol. Chem. **271:** 3488–3495.

Kim, Y. H., C. Y. Choi, S. J. Lee, M. A. Conti and Y. Kim, 1998 Homeodomain-interacting protein kinases, a novel family of co-repressors for homeodomain transcription factors. J. Biol. Chem. **273:** 25875–25879.

Mello, C. C., J. M. Kramer, D. Stinchcomb and V. Ambros, 1991 Efficient gene transfer in C. elegans: extrachromosomal maintenance and integration of transforming sequences. EMBO J. **10:** 3959–3970.

Shindoh, N., J. Kudoh, H. Maeda, A. Yamaki, S. Minoshima *et al.*, 1996 Cloning of a human homolog of the Drosophila minibrain/rat Dyrk gene from "the Down syndrome critical region" of chromosome 21. Biochem. Biophys. Res. Commun. **225:** 92–99.

Smith, D. J., M. E. Stevens, S. P. Sudanagunta, R. T. Bronson, M. Makhinson *et al.*, 1997 Functional screening of 2 Mb of human chromosome 21q22.2 in transgenic mice implicates minibrain in learning defects associated with Down syndrome. Nat. Genet. **16:** 28–36.

Song, W. J., S. H. Chung and D. M. Kurnit, 1997 The murine Dyrk protein maps to chromosome 16, localizes to the nucleus, and can form multimers. Biochem. Biophys. Res. Commun. **231:** 640–644.

Takashima, S., 1997 Down syndrome. Curr. Opin. Neurol. **10:** 148–152.

Tejedor, F., X. R. Zhu, E. Kaltenbach, A. Ackermann, A. Baumann *et al.*, 1995 minibrain: a new protein kinase family involved in postembryonic neurogenesis in Drosophila. Neuron **14:** 287–301.

Timmons, L., D. L. Court and A. Fire, 2001 Ingestion of bacterially expressed dsRNAs can produce specific and potent genetic interference in Caenorhabditis elegans. Gene **263:** 103–112.

Troemel, E. R., A. Sagasti and C. I. Bargmann, 1999 Lateral signaling mediated by axon contact and calcium entry regulates asymmetric odorant receptor expression in C. elegans. Cell **99:** 387–398.

Yu, S., L. Avery, E. Baude and D. L. Garbers, 1997 Guanylyl cyclase expression in specific sensory neurons: a new family of chemosensory receptors. Proc. Natl. Acad. Sci. USA **94:** 3384–3387.

Communicating editor: B. J. Meyer